Manufacturing & Service Operations Management

Publication details, including instructions for authors and subscription information:
http://pubsonline.informs.org

From Curtailed Renewable Energy to Green Hydrogen: Infrastructure Planning for Hydrogen Fuel-Cell Vehicles

Long He, Nan Ke, Ruijiu Mao, Wei Qi, Hongcai Zhang

To cite this article:
Long He, Nan Ke, Ruijiu Mao, Wei Qi, Hongcai Zhang (2024) From Curtailed Renewable Energy to Green Hydrogen: Infrastructure Planning for Hydrogen Fuel-Cell Vehicles. Manufacturing & Service Operations Management

Published online in Articles in Advance 07 Aug 2024

. https://doi.org/10.1287/msom.2022.0381

MANUFACTURING & SERVICE OPERATIONS MANAGEMENT
Articles in Advance, pp. 1–18
ISSN 1523-4614 (print), ISSN 1526-5498 (online)
https://pubsonline.informs.org/journal/msom

From Curtailed Renewable Energy to Green Hydrogen: Infrastructure Planning for Hydrogen Fuel-Cell Vehicles

Long He,[a] Nan Ke,[b] Ruijiu Mao,[b] Wei Qi,[c,*] Hongcai Zhang[d,*]

[a] School of Business, The George Washington University, Washington, District of Columbia 20052; [b] Institute of Operations Research and Analytics, National University of Singapore, Singapore 117602; [c] Department of Industrial Engineering, Tsinghua University, Beijing 100084, China; [d] Department of Electrical and Computer Engineering, University of Macau, Macau 999078, China

*Corresponding authors

Contact: longhe@gwu.edu, https://orcid.org/0000-0002-9951-7450 (LH); nan.ke@u.nus.edu, https://orcid.org/0009-0000-9560-2431 (NK); maoruijiu@u.nus.edu, https://orcid.org/0000-0001-9941-0744 (RM); qiw@tsinghua.edu.cn, https://orcid.org/0000-0003-3948-835X (WQ); hczhang@um.edu.mo, https://orcid.org/0000-0002-8294-6419 (HZ)

Received: August 5, 2022
Revised: February 19, 2024; May 29, 2024
Accepted: June 30, 2024
Published Online in Articles in Advance: August 7, 2024

https://doi.org/10.1287/msom.2022.0381

Abstract. ***Problem definition*:** Hydrogen fuel-cell vehicles (HFVs) have been proposed as a promising green transportation alternative. For regions experiencing renewable energy curtailment, promoting HFVs can achieve the dual benefit of reducing curtailment and developing sustainable transportation. However, promoting HFVs faces several major hurdles, including uncertain vehicle adoption, the lack of refueling infrastructure, the spatial mismatch between hydrogen demand and renewable sources for hydrogen production, and the strained power transmission infrastructure. In this paper, we address these challenges and study how to promote HFV adoption by deploying HFV infrastructure and utilizing renewable resources. ***Methodology/results*:** We formulate a planning model that jointly determines the location and capacities of hydrogen refueling stations (HRSs) and hydrogen plants as well as electricity transmission and grid upgrade. Despite the complexity of explicitly considering drivers' HFV adoption behavior, the bilevel optimization model can be reformulated as a tractable mixed-integer second-order cone program. We apply our model calibrated with real data to the case of Sichuan, a province in China with abundant hydro resources and a vast amount of hydropower curtailment. ***Managerial implications*:** We obtain the following findings. (i) The optimal deployment of HRSs displays vastly different spatial patterns depending on the HFV adoption target. The capital city, a transportation hub, is excluded from the plan under a low target and only emerges as the center of HFV adoption under a high target. (ii) Promoting the HFV adoption can overall help reduce hydropower curtailment, but the effectiveness depends on factors such as the adoption target and the grid upgrade cost. (iii) Being a versatile energy carrier, hydrogen can be transported to various locations, which allows for strategic placement of HRSs in locations distinct from hydrogen plant sites. This flexibility offers HFVs greater potential cost savings and curtailment reduction compared with other alternative fuel vehicles (e.g., electric vehicles) under current cost estimates.

Funding: W. Qi acknowledges the support from the National Natural Science Foundation of China [Grants 72242106 and 72188101] and the Natural Sciences and Engineering Research Council of Canada [Grant RGPIN-2019-04769].

Supplemental Material: The online appendix is available at https://doi.org/10.1287/msom.2022.0381.

Keywords: hydrogen fuel-cell vehicles • infrastructure planning • green transportation • power systems

1. Introduction

Hydrogen has gained rapidly growing attention around the globe in recent years as the world is combating climate change and transitioning toward a more sustainable future. As a versatile energy carrier and chemical feedstock, hydrogen can be used in a variety of applications across the manufacturing, transport, power, and building sectors. Consuming hydrogen produces no carbon dioxide (CO_2) or harmful substance—ideal for reducing greenhouse emissions and air pollution from these sectors. With the advancement in hydrogen technologies, the declining cost of renewable energy, and the urgency to reduce greenhouse gas emissions, hydrogen is expected to be a key component in the energy system of the future. For instance, in the European Union's strategic vision for a climate-neutral economy, the share of hydrogen in Europe's energy mix is projected to grow from less than 2% in 2020 to 13%–14% by 2050 (European Commission 2018). To realize the full potential of hydrogen, many countries and economies, such as the United States, the European Union, and China, have announced their official strategies in

support of developing the hydrogen industry (European Commission 2020, U.S. Department of Energy 2020, Xinhuanet 2022).

Several global initiatives mentioned above actively promote hydrogen fuel-cell vehicles (HFVs), recognizing them as one of the most promising green transportation alternatives. HFVs, powered by electricity generated through the reaction of hydrogen with oxygen in a fuel cell, generally have higher overall efficiency compared with fossil fuel vehicles and emit no air pollutants (U.S. Department of Energy 2021). Given these merits, major automobile manufacturers are competing in the development of HFV models, such as Toyota Mirai, Hyundai Nexo, Honda Clarity, and BMW i Hydrogen NEXT. Despite this, the prevailing belief is that the future of small passenger vehicles lies in battery electric vehicles (EVs). HFVs, on the other hand, are deemed more advantageous for long-distance, heavy commercial transportation (Timperley 2021). Notably, HFV trucks can provide extended driving ranges exceeding 800 kilometers (km) and can be refueled in 5–20 minutes (e.g., Hyzon Motors 2023, Nikola 2023b). When used on the scale required for trucking, the EV batteries become heavy and consequently, diminish profits in freight transportation (Toyota 2022). Additionally, it is anticipated that the hydrogen refueling cost will continue to decrease as more hydrogen refueling stations (HRSs) become available (BAE Systems 2021).

In addition to the environmental advantages on the demand side, HFVs can contribute to enhancing the penetration of renewable energy and mitigating its curtailment from the supply side. As an appropriate energy carrier for variable renewable resources, like hydro, solar, and wind (International Renewable Energy Agency 2021), hydrogen (produced with electricity) can be utilized to reduce energy curtailment that arises when electricity supply surpasses demand or transmission constrained by grid capacity. We consider water electrolysis as the method of hydrogen production, which splits water into hydrogen and oxygen using electricity. When the electricity used in this process is generated from renewable or low-carbon sources, the hydrogen produced is referred to as the *green hydrogen* (Dincer 2012). Figure 1 illustrates a hydrogen supply chain encompassing electricity transmission, hydrogen production, and distribution. To supply the required power for water electrolysis, electricity is transmitted from power plants to hydrogen plants through the grid. The generated hydrogen is subsequently transported to hydrogen refueling stations in designated regions using methods such as tube trailers or pipelines. When feasible, utilizing tube trailers powered by hydrogen, such as through HFV trucks, and repurposing existing natural gas pipelines for hydrogen transport will be more cost effective and eco-friendly.

Recognizing the benefits of HFVs from both the demand side (e.g., reducing tailpipe emissions) and the supply side (e.g., mitigating energy curtailment), many governments emphasize the promotion of HFVs in their hydrogen initiatives. For instance, the government of Sichuan, a province in southwest China abundant in hydropower resources, regards HFVs as a significant opportunity in its hydrogen plan (Sichuan Provincial Economic and Information Department 2020). Given the substantial hydropower curtailment because of constrained grid transmission capacity (e.g., 20 terawatt-hours (TWh) in 2020) (Sixth Tone 2022), promoting HFVs in Sichuan Province has the potential to yield dual benefits by mitigating hydropower spillage and fostering the development of green transportation.

However, the promotion of HFVs encounters significant challenges in the design of the hydrogen supply chain network. First, on the supply side, over 95% of today's hydrogen is produced from fossil fuels by steam reforming of natural gas, partial oxidation of methane, and coal gasification, which are not economical for providing fuels for HFVs and entail substantial CO_2 emissions (International Renewable Energy Agency 2021). To make it cost competitive and sustainable, the most promising approach is to produce hydrogen through water electrolysis, with electricity generated from inexpensive renewable sources (e.g., the otherwise curtailed hydropower). Hence, locating hydrogen plants should be coordinated with the utilization of curtailed hydropower. Second, on the demand side, the strategic placement of hydrogen refueling stations plays a crucial role in facilitating the widespread adoption of HFVs (Chen et al. 2021). This adoption-promoting effect is particularly pronounced in the early stage when the HRS infrastructure is scarce, such as is the current situation in Sichuan Province. As of January 2024, only five HRSs are available (Glpautogas Info 2024). The challenge is aggravated by the spatial mismatch between demand areas and renewable energy sources. In Sichuan Province, the

Figure 1. (Color online) The Hydrogen Supply Chain

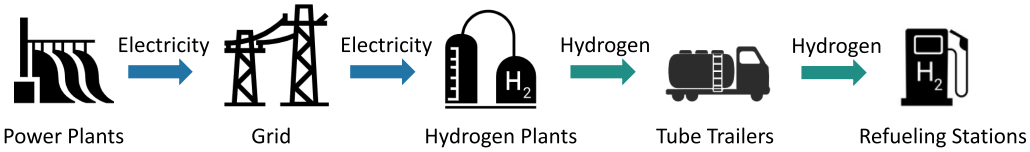

hydropower curtailment mainly occurs in the province's southwest, whereas the population is concentrated predominantly in the east (see Figure 2). This spatial mismatch adds complexity to the decision making faced by system planners as they grapple with determining the optimal location for hydrogen production—whether it should be closer to the water curtailment source or the demand market. Third, the substantial electricity demand for large-scale hydrogen production through water electrolysis has the potential to strain the grid. Consequently, planners must take into account the necessity for grid upgrades when designing the hydrogen supply chain network.

In light of these promises and challenges of HFVs, this paper investigates how we can promote HFV adoption by designing the hydrogen supply chain network and utilizing otherwise curtailed renewable energy. Taking the perspective of a social planner, the objective is to achieve a prespecified target level of HFV adoption measured by vehicle miles traveled (VMT) while minimizing the total infrastructure investment and operating cost. Our paper proposes an integrated model of the hydrogen supply chain network design to jointly determine the locations and capacities of HRSs and hydrogen plants as well as the capacity upgrade and the loading of the electric power grid (assuming exogenous power generation). Through a case study based on the real data of Sichuan Province, we aim to understand how to better design HFV infrastructures under various practical conditions. Moreover, we investigate when HFVs emerge as a viable alternative in comparison with EVs, aiming to promote green transportation and mitigate energy curtailment simultaneously. Here, we outline our primary contributions in tackling the challenges mentioned above.

Figure 2. (Color online) The Spatial Mismatch Between Population and Hydropower Curtailment of Sichuan Province

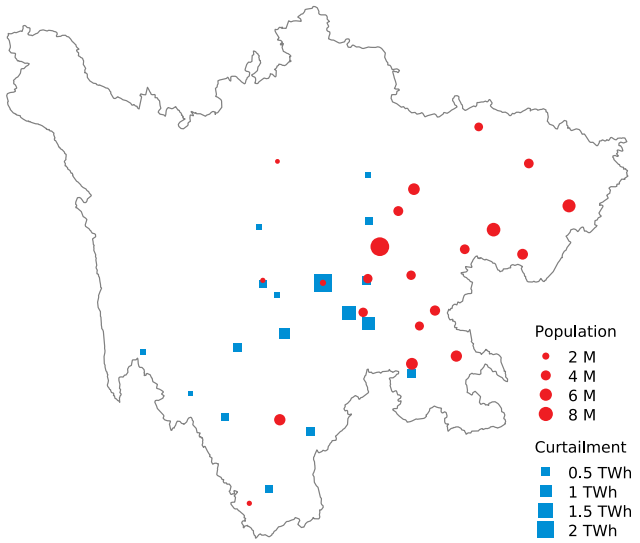

- Our model comprehensively incorporates crucial and interconnected factors in the hydrogen supply chain, encompassing HFV adoption and usage, hydrogen production and distribution, electricity transmission, and grid upgrades.
- We explicitly take into account HFV adoption that depends on the deployment of HRSs in the network. This leads to a bilevel optimization problem that can be reformulated into a mixed-integer second-order cone program (MISOCP). Our approach effectively addresses the exact reformulation of worst-case adoption rates (the equality chance constraint) as the ratio of two quadratic functions, distinguishing our approach from earlier work that only reformulates the relaxed bound (the inequality chance constraint) on the worst-case adoption rate (e.g., El Ghaoui et al. 2003, He et al. 2017). Our techniques can potentially be applied to other problems to handle equality constraints involving ratios of two quadratic functions.
- Our computational studies using real data on the case of Sichuan Province offer managerial insights on the design of the hydrogen supply chain for HFV adoption and energy curtailment reduction.

1. The VMT target significantly influences network design decisions. In the case of Sichuan Province, when the VMT target is low, hydrogen production is situated near hydropower curtailment sources, where the demand market, although modest, is adequate to meet the VMT target. In contrast, with a high VMT target, the network expands to include Chengdu, the capital city of the province, boasting the largest HRS capacity and the highest HFV adoption.
2. The promotion of HFVs can contribute to an overall reduction in hydropower curtailment, although the effectiveness varies depending on the VMT target and factors, such as grid upgrade costs and electricity purchase prices. Particularly, when the electricity purchase price is low, the curtailment reduction experiences only marginal increases with the VMT target after reaching a certain level. Therefore, to attain the dual benefits of minimizing hydropower spillage and fostering green transportation, planners should meticulously assess these factors and select an appropriate level for the HFV adoption target.
3. Amidst the ongoing debate regarding the promotion of EVs versus HFVs as sustainable solutions for green transportation and mitigating energy curtailment, our investigation reveals that EVs hold an advantage when the costs associated with hydrogen transportation and/or HRSs are higher, particularly under high a VMT target. However, based on current cost estimates, HFVs emerge as the more cost-effective option because of the flexibility of hydrogen transport, enabling

strategic placement of HRSs in locations separate from hydrogen production sites within the supply chain. In contrast, EVs rely solely on chargers powered by the grid, thereby limiting their ability to fully utilize curtailed renewable energy under grid constraints. Consequently, for freight transport, advocating for HFV trucks presents greater cost savings and curtailment reduction potential compared with EV trucks at the present stage.

The rest of this paper is organized as follows. Section 2 reviews the related literature. Section 3 describes the optimization model for planning HFV infrastructures. Section 4 applies the model to the case of Sichuan Province, and it also develops managerial insights based on the computational studies. Finally, Section 5 concludes the paper.

2. Literature Review

Infrastructure planning for HFVs is by nature a crossdisciplinary research problem because of intertwined factors, such as vehicle adoption, fuel distribution, and power grid operations. Thus, our work lies at the interface of multiple academic fields, including operations management, transportation, and power systems. Below, we review the related literature in these fields.

Planning supporting infrastructure for alternative fuel vehicles (AFVs) is vital for its mass adoption, and it has attracted growing interest from operations management and transportation communities. The majority of this literature considers EVs with plug-in charging (e.g., He et al. 2021, Zhang et al. 2021) or battery swapping (e.g., Mak et al. 2013, Avci et al. 2015, Qi et al. 2023). However, models and insights from those studies cannot be directly applied to the context of HFVs. Refueling HFVs does not involve charging or battery swapping, but rather, it requires hydrogen that is produced at hydrogen plants using certain resources (e.g., electricity in our work) and then delivered to the HRSs to meet demand. Such a different fuel supply process leads to new design challenges, such as hydrogen plant location and fuel distribution, which our model explicitly addresses.

Researchers in the transportation field have also studied the refueling station location problems for generic AFVs and HFVs. In the context of generic AFVs, Kuby and Lim (2005) develop a flow-refueling location model to locate refueling facilities, accounting for the limited range of AFVs. Further research extends this model by locating stations along arcs of the transportation network (Kuby and Lim 2007) or by introducing path deviation tolerance of the drivers (Arslan et al. 2019). Bhatti et al. (2015) propose and solve a two-stage AFV refueling station location problem featuring an option to open more stations in the second stage after demand learning. In the context of HFVs, the literature commonly considers exogenous vehicle travel demand (Kang and Recker 2015, Brey et al. 2016). However, the volume and pattern of AFV flows are likely to be affected by the deployment of refueling facilities, especially in the early stage of adoption, which is the case of HFVs. To address this issue, Mahmutoğulları and Yaman (2023) maximize the flows of refueled alternative fuel vehicles, taking into account vehicle range limitations and drivers' willingness to deviate for refueling. The authors introduce the robust counterpart of the refueling station location problem, incorporating the decision-dependency flow uncertainty set. Although sharing a similar spirit of considering drivers' willingness of deviation, we instead use a distributional robust optimization approach in characterizing HFV adoption using the mean and covariance information of drivers' random utility. Furthermore, our study addresses the design of the hydrogen supply chain network, incorporating the power system with the dual objective of advancing green transportation and mitigating energy curtailment.

The mobility system of AFVs is naturally interrelated with the power system because the grid is a major energy provider for AFVs. Yet, the literature of operation management and transportation has largely ignored the power grid when planning AFV infrastructures. Among very few exceptions, Qi et al. (2022) study the potential of shared autonomous EVs for enhancing the self-efficiency and resilience of solar-powered urban microgrids. Zhang et al. (2021) consider vehicle-to-grid electricity selling when planning an EV-sharing system and discuss its benefit for service providers, customers, the environment, and the electrical grid. However, all of these works abstract away important grid characteristics, such as the network structure and power flow constraints. In contrast, using a direct current (DC) power flow model from the power system literature and real grid data, our work models electricity transmission in detail and accounts for the necessary grid upgrades in support of hydrogen production, aiming to better capture the interconnection between transportation and power systems. For reviews of the DC power flow model and its application on transmission planning, we refer readers to both Stott et al. (2009) and Hemmati et al. (2013).

Finally, our paper also relates to a line of works in the power system literature that study the coupling between transportation systems and electrical grid networks. For instance, Yang et al. (2014) study day-ahead scheduling and real-time dispatch for plug-in EVs. Yao et al. (2014) consider jointly planning a power distribution system and EV charging facilities using a multiobjective optimization model to maximize the captured traffic flow. Alizadeh et al. (2016) study the impact of introducing a large number of EVs on power and transportation networks, and then, they propose a scheme to coordinate independent operators of these two networks toward

the socially optimal operating point. Zhang et al. (2017) propose a mathematical programming model to locate hydrogen refueling stations on a highway network, which considers grid reinforcement for supporting on-site hydrogen production. However, none of these works adequately address important behavior issues, such as endogenous vehicle adoption and drivers' route choice, which are central for promoting HFVs and a major focus of this paper.

3. Hydrogen Supply Chain Network Design

We consider a social planner who aims to promote HFVs by configuring the hydrogen supply chain network design and utilizing hydropower curtailment in a collection of regions. The goal of the planner is to achieve a prespecified level of HFV adoption, measured by VMT, at the minimum cost that consists of infrastructure investment and operating cost. To that end, the planner needs to decide which regions to serve such that the total HFV adoption level would meet the target. Also, the planner needs to build hydrogen plants and upgrade the supporting electricity transmission grid such that the hydrogen demand can be fulfilled in a cost-effective way. Below, we first describe the models of HFV adoption and hydrogen demand in Section 3.1 followed by the hydrogen production and transportation modeling in Section 3.2 and the integrated optimization model in Section 3.3. A notational summary is available in Online Appendix A.

3.1. HFV Adoption and Hydrogen Demand

Suppose the planner considers deploying hydrogen refueling stations in a set I of nonoverlapping geographical regions (e.g., cities). We use binary decision variables x_i for $i \in I$ to indicate whether the planner chooses to build any HRS in region i ($x_i = 1$) or not ($x_i = 0$). If region i is chosen, the planner further decides the total (refueling) capacity of the hydrogen refueling stations y_i (kilograms (kg) per day) in this region.

For the scope of this study, we consider the set of round trips for drivers residing in region i. When the driver travels within region i, it is considered a round trip with both the origin and destination being i, represented by (i, i). If the driver travels to a sequence of destination regions $i_1, \ldots, i_n$ distinct from i, the entire trip along with the return trip to region I is considered a round trip denoted by $(i, i_1, \ldots, i_n, i)$. Define T_i as the collection of trips that drivers residing in region i can undertake, and let $T = \cup_{i \in I} T_i$ represent the overall set of trips. In the subsequent exposition, unless explicitly stated otherwise, all trips are considered round trips.

As discussed in earlier works (e.g., Kim and Kuby 2012, Arslan et al. 2019, Mahmutoğulları and Yaman 2023), drivers may deviate from their shortest paths of a trip for refueling. We then define an *HFV route* as the sequence of regions denoted by r. This route includes the destinations listed in trip t as well as required HRS stops $S_{tr} \subseteq I$ that the driver visits to fulfill a trip. As explained below, the feasibility of an HFV route depends on the existence of HRSs in S_{tr}. For trip $t \in T$, we denote R_t by the set of such routes. For each route r, we denote the route length as l_r. In Online Appendix B.1, we show the construction of sets R_t and S_{tr} based on the HFV range.

Note that whether a driver can take an HFV route is contingent upon the presence of the required HRS. That is, the route r is a *feasible HFV route* for trip t only if $x_k = 1$ for all $k \in S_{tr}$. Additionally, we assume that the driver opts for the shortest feasible HFV route if available; otherwise, they choose an alternative travel mode. Such a route choice can be established by solving the following Problem (1) given HRS locations $\boldsymbol{x}$:

$$(w_{tr})_{r \in R_t \cup \{0\}} = \arg\min_{\omega_{tr} \in \{0,1\}} \left\{ \sum_{r \in R_t} l_r \omega_{tr} + \bar{l}_t \omega_{t0} : \sum_{r \in R_t} \omega_{tr} + \omega_{t0} = 1; \; \omega_{tr} \le x_k, \; \forall k \in S_{tr} \right\}, \quad \forall t \in T, \tag{1}$$

where binary variable $w_{tr} \in \{0, 1\}$ indicates whether drivers choose HFV route $r \in R_t$ for trip t , binary variable $w_{t0} \in \{0, 1\}$ indicates whether drivers choose an alternative mode for trip t, and the parameter $\bar{l}_t > \max_{r \in R_t} l_r$ denotes the penalty for the nonexistence of a feasible HFV route (e.g., the driver needs to choose an alternative mode). In Problem (1), if there exists a feasible HFV route for trip t, Problem (1) finds a feasible HFV route with the shortest length. If there is no feasible HFV route, Problem (1) returns $w_{t0} = 1$. The first set of constraints ensures that the drivers choose only one HFV route or the alternative mode. The second set of constraints requires that a route be chosen only if it is a feasible HFV route.

3.1.1. HFV Adoption. We characterize how the drivers decide on the adoption of HFVs in the presence of HRS deployment design $\boldsymbol{x}$. Let q_i denote the adoption rate in region I (i.e., the portion of drivers choose to use HFVs). We first assume that drivers in region i would adopt HFVs only if there is an HRS available in this region: that is,

$$q_i \le x_i, \quad \forall i \in I. \tag{2}$$

We next consider the following satisficing behavior of HFV adoption. A key consideration for the driver considering HFV adoption is the convenience of accessing destination regions without necessitating substantial detours. These detours might be required because of the limited availability of HRSs and the HFV's range. For prospective HFV users situated in region i, the

assessment of accessibility to a destination region j pertains to the round trip $t = (i, j, i)$. Specifically, we introduce a binary variable ϕ_{ij} that indicates whether drivers in region i can travel to region j and return home using HFVs within a tolerance limit γ for the route deviation (Kim and Kuby 2012, Arslan et al. 2019, Mahmutoğulları and Yaman 2023). In other words, $\phi_{ij} = 1$ when there exists a route $r \in R_{(i,j,i)}$ such that $l_r \le (1+\gamma)d_{ij}$, where d_{ij} is the round-trip distance between regions i and j. To this end, we introduce the constraints for ϕ_{ij} below:

$$\sum_{r\in R_{(i,j,i)}} l_r w_{(i,j,i)r} + \bar{l}_{(i,j,i)}(w_{(i,j,i)0} + \phi_{ij} - 1) \le (1+\gamma)d_{ij}, \quad \forall i,j \in I, i \ne j, \tag{3a}$$

$$(1+\gamma)d_{ij} \le \sum_{r\in R_{(i,j,i)}} l_r w_{(i,j,i)r} + \bar{l}_{(i,j,i)}(w_{(i,j,i)0} + \phi_{ij}), \quad \forall i,j \in I, i \ne j, \tag{3b}$$

$$\phi_{ii} = x_i, \quad \forall i \in I, \tag{3c}$$

$$\phi_{ij} \in \{0,1\}, \quad \forall i,j \in I, \tag{3d}$$

where the parameter $\bar{l}_{(i,j,i)} > \max\{(1+\gamma)d_{ij}, \max_{r\in R_{(i,j,i)}} l_r\}$. We can verify that if there is no feasible HFV route in Problem (1), we have $\sum_{r\in R_{(i,j,i)}} l_r w_{(i,j,i)r} = 0$ and $w_{(i,j,i)0} = 1$, which leads to $\phi_{ij} = 0$ by Constraint (3a). If there exists a feasible HFV route (i.e., $w_{(i,j,i)0} = 0$), then $\phi_{ij} = 0$ when $\sum_{r\in R_{(i,j,i)}} l_r w_{(i,j,i)r} > (1+\gamma)d_{ij}$ by Constraint (3a) and $\phi_{ij} = 1$ when $\sum_{r\in R_{(i,j,i)}} l_r w_{(i,j,i)r} \le (1+\gamma)d_{ij}$ by Constraint (3b). Finally, by definition, region i is accessible if there is an HRS (i.e., $\phi_{ii} = x_i$).

Following the satisficing decision-making criteria (e.g., Simon 1957, He et al. 2017), we assume that a driver would adopt an HFV if the total utility from adopting an HFV exceeds an aspiration level b_i. If region j is accessible by an HFV within the deviation limit γ, the driver residing in region i would enjoy utility a_{ij}, a random value that may depend on the frequency and value of these traveling records. Naturally, drivers are heterogenous in their utility values for trips. We can thus view the utility vector $\boldsymbol{a}_i = [a_{ij}]_{j\in I}$ as a random vector that follows an underlying distribution $\mathbb{P}$. The utility vector of each driver in region i can be seen as a sample independently drawn from $\mathbb{P}$. Thus, at the aggregate level, we can express the adoption rate as $\mathbb{P}[\sum_{j\in I} a_{ij}\phi_{ij} \ge b_i]$.

To evaluate this probability, the planner needs the complete information about $\mathbb{P}$: the joint probability distribution of trip utility $\boldsymbol{a}_i = [a_{ij}]_{j\in I}$ for all $i \in I$. However, such perfect information is usually difficult, if not impossible, to obtain, especially in the planning stage when only limited data may be available (e.g., from surveys). Nevertheless, partial information on $\boldsymbol{a}_i$ (e.g., its mean and covariance matrix) is relatively easy to acquire. Therefore, we take the view from distributionally robust optimization with known mean $\boldsymbol{\mu}_i = [\mu_{ij}]_{j\in I}$ and covariance matrix $\boldsymbol{\Sigma}_i = [\sigma_{(ij_1)(ij_2)}]_{j_1,j_2\in I}$ of utility vector $\boldsymbol{a}_i$, which is a popular and practical setting in distributionally robust optimization (see, for example, El Ghaoui et al. 2003, Delage and Ye 2010, and He et al. 2017). The planner considers an ambiguity set $\mathcal{P}_i$ consisting of all distributions of $\boldsymbol{a}_i$ with that same mean $\boldsymbol{\mu}_i$ and covariance matrix $\boldsymbol{\Sigma}_i$, and then, the planner plans against the one from $\mathcal{P}_i$ that gives the worst-case (i.e., the lowest) HFV adoption rate. Then, together with (2), we can express q_i as the worst-case adoption rate:

$$q_i = \begin{cases} \inf\limits_{\mathbb{P}\in\mathcal{P}_i} \mathbb{P}\left[\sum\limits_{j\in I} a_{ij}\phi_{ij} \ge b_i\right], & \text{if } x_i = 1, \\ 0, & \text{otherwise.} \end{cases} \tag{4}$$

We obtain an explicit expression for the adoption rate Constraint (4) below as a direct result from El Ghaoui et al. (2003) and He et al. (2017).

Lemma 1. *Constraint* (4) *is equivalent to the following*:

$$q_i = \begin{cases} \dfrac{(\boldsymbol{\mu}_i^T\boldsymbol{\phi}_i - b_i)^2}{\boldsymbol{\phi}_i^T\boldsymbol{\Sigma}_i\boldsymbol{\phi}_i + (\boldsymbol{\mu}_i^T\boldsymbol{\phi}_i - b_i)^2}, & \text{if } \boldsymbol{\mu}_i^T\boldsymbol{\phi}_i \ge b_i \text{ and } x_i = 1, \\ 0, & \text{otherwise,} \end{cases} \tag{5}$$

where $\boldsymbol{\phi}_i = [\phi_{ij}]_{j\in I}$.

We can see from Lemma 1 that the adoption rate in region i is nonzero only when HRSs are deployed in this region, and the mean utility of adopting an HFV exceeds the aspiration level. Before proceeding, we would like to remark on our adoption rate model, which is related to the adoption rate model for the EV-sharing customers in He et al. (2017). First, both works model endogenous adoption behavior via drivers' utility. In He et al. (2017), customers' utility derived from adopting EV-sharing service directly depends on the coverage of service regions. Factors like vehicle range and drivers' route choice, which might be important in practice, are not considered. In contrast, in our study, the driver's utility is contingent on the accessibility of destinations by HFVs, constrained by the range of HFVs and influenced by the deployment of HRS. Second, both works consider the worst-case adoption rate among all distributions of the utility $\boldsymbol{a}_i$ in the ambiguity set $\mathcal{P}_i$. However, He et al. (2017) relax the worst-case adoption rate constraint as an inequality (e.g., see He et al. 2017, constraint 4 on p. 314), and in the optimal solution, q_i is not guaranteed to be the worst-case adoption rate. By contrast, in our work, q_i must be *exactly* equal to the worst-case adoption rate (see Constraint (4)), which eliminates the potential gap. This equality constraint introduces additional difficulty because it cannot be directly represented as a second-order cone (SOC) constraint as in El Ghaoui et al. (2003) or He et al. (2017), which relies on the *inequality* such that their reformulation only needs one set of second-order cone constraints. In our case, however, Proposition 1

shows that this equality Constraint (5) can still be reformulated by two sets of SOC constraints and using proper linearization techniques.

Proposition 1. *Constraint* (5) *is equivalent to the following set of constraints*:

$$b_i u_i \le \sum_{j\in I} \mu_{ij}\phi_{ij}, \quad \forall i \in I, \tag{6a}$$

$$\sum_{j\in I} \mu_{ij}\phi_{ij} \le \sum_{j\in I} \mu_{ij}u_i + b_i, \quad \forall i \in I, \tag{6b}$$

$$\left\| \begin{matrix} q_i - \beta_i \\ 2\alpha_i \end{matrix} \right\|_2 \le q_i + \beta_i, \quad \forall i \in I, \tag{6c}$$

$$\left\| \begin{matrix} -q_i - \beta_i \\ 2\boldsymbol{\Sigma}_i^{1/2}\boldsymbol{\phi}_i \end{matrix} \right\|_2 \le 1 - q_i + \beta_i, \quad \forall i \in I, \tag{6d}$$

$$\alpha_i = \sum_{j\in I} \mu_{ij}\epsilon_{ijj} - b_i v_i, \quad \forall i \in I, \tag{6e}$$

$$\beta_i = \sum_{j_1\in I}\sum_{j_2\in I} \sigma_{(ij_1)(ij_2)}\delta_{ij_1j_2} + \sum_{j_1\in I}\sum_{j_2\in I} \mu_{ij_1}\mu_{ij_2}\epsilon_{ij_1j_2} + b_i^2 v_i - 2b_i\sum_{j\in I}\mu_{ij}\epsilon_{ijj}, \quad \forall i \in I, \tag{6f}$$

$$u_i \in \{0,1\}, \quad \forall i \in I, \tag{6g}$$

$$(v_i, x_i, u_i) \in \mathcal{A}, \quad \forall i \in I, \tag{6h}$$

$$(\delta_{ij_1j_2}, \phi_{ij_1}, \phi_{ij_2}) \in \mathcal{A}, \quad \forall i, j_1, j_2 \in I, \tag{6i}$$

$$(\epsilon_{ij_1j_2}, v_i, \phi_{ij_1}, \phi_{ij_2}) \in \mathcal{B}, \quad \forall i, j_1, j_2 \in I, \tag{6j}$$

where $u_i, v_i, \alpha_i, \beta_i, \delta_{ij_1j_2}, \epsilon_{ij_1j_2}$ *are auxiliary decision variables and where* $\mathcal{A}$ *and* $\mathcal{B}$ *are feasible regions characterized by linear constraints to be provided in* (7) *and* (8), *respectively*:

$$\mathcal{A} = \{(v,x,u) \in \{0,1\}^3 : v \ge 0, v \le x, v \le u, v \ge x + u - 1\}, \tag{7}$$

$$\mathcal{B} = \{(v,x,y,z) \in \{0,1\}^4 : v \ge 0, v \le x, v \le y, v \le z, v \ge x + y + z - 2\}. \tag{8}$$

3.1.2. Hydrogen Refueling Demand.

Now, we can connect the HFV adoption and drivers' route choices with hydrogen demand. Suppose parameter N_t is the potential rate of trip $t \in T_i$ with origin/destination in region I; the realized rate of trip t would be $N_t q_i$. Let parameter η_{rk} be the amount of hydrogen refueled in region $k \in I$ when a driver travels along route r ($\eta_{rk} = 0$ if k is not in route r). By the definition of w_{tr} in the route choice model in (1), a single trip t would generate $\sum_{r\in R_t}\eta_{rk}w_{tr}$ amount of hydrogen demand in region k. Hence, the total hydrogen demand D_k in region $k \in I$ can be written as $D_k = \sum_{i\in I}\sum_{t\in T_i} N_t q_i \sum_{r\in R_t}\eta_{rk}w_{tr}$. By replacing the bilinear term $q_i w_{tr}$ with variable κ_{tr}, we can express this equation as the following constraint:

$$D_k = \sum_{t\in T}\sum_{r\in R_t} N_t \eta_{rk}\kappa_{tr}, \quad \forall k \in I. \tag{9}$$

Furthermore, for $t \in T_i$, we enforce $\kappa_{tr} = q_i w_{tr}$ using the following set of constraints:

$$\kappa_{tr} \ge 0, \quad \forall i \in I, t \in T_i, r \in R_t, \tag{10a}$$

$$\kappa_{tr} \le q_i, \quad \forall i \in I, t \in T_i, r \in R_t, \tag{10b}$$

$$\kappa_{tr} \le w_{tr}, \quad \forall i \in I, t \in T_i, r \in R_t, \tag{10c}$$

$$\kappa_{tr} \ge q_i + w_{tr} - 1, \quad \forall i \in I, t \in T_i, r \in R_t. \tag{10d}$$

To fulfill the demand, the decision of the refueling capacity in each region i, y_i (kilograms per day), should be no less than the hydrogen demand: that is,

$$D_i \le y_i, \quad \forall i \in I. \tag{11}$$

Let Y_i be the maximum total capacity of HRSs allowed in region i. The following constraint ensures that no HRS will be deployed unless region i is selected:

$$y_i \le Y_i x_i, \quad \forall i \in I. \tag{12}$$

Recall that the planner wishes to achieve a target level of HFV adoption measured by VMT. Let $\Gamma \in [0,1]$ be the VMT target, which is the percentage of VMT by HFVs. Suppose that s_t is the average mileage per trip t and that $o(t)$ is the origin (and the destination) of trip t. The VMT target constraint can be written as

$$\sum_{i\in I} q_i \sum_{t:o(t)=i} N_t \sum_{r\in R_t} l_r w_{tr} \ge \Gamma\left(\sum_{i\in I}(1-q_i)\sum_{t:o(t)=i} s_t N_t + \sum_{i\in I} q_i \sum_{t:o(t)=i} N_t \sum_{r\in R_t} l_r w_{tr}\right),$$

where the left-hand side is the total realized VMT and the right-hand side is the target Γ times the total VMT that can be potentially achieved by a combination of conventional vehicles and HFVs. Note that $\kappa_{tr} = q_i w_{tr}$. We can reformulate the VMT constraint as

$$(1-\Gamma)\sum_{i\in I}\sum_{t:o(t)=i} N_t \sum_{r\in R_t} l_r \kappa_{tr} \ge \Gamma\sum_{i\in I}(1-q_i)\sum_{t:o(t)=i} s_t N_t. \tag{13}$$

To summarize, this subsection models the relationship between the HRS deployment decision $\boldsymbol{x}$ and drivers' route choices, HFV adoption, and hydrogen demand. In what follows, we discuss how the planner can set up a hydrogen supply chain so as to fulfill the hydrogen demand efficiently.

3.2. Hydrogen Production/Transportation Joint with Grid Upgrade

To set up this hydrogen supply chain as illustrated in Figure 1, the planner needs to deploy hydrogen plants at appropriate locations. In addition, to support the electricity transmission for hydrogen production, parts of the existing transmission lines need to be upgraded to avoid line overloading. To achieve cost efficiency for the hydrogen supply chain, the locations of hydrogen plants

need to be carefully decided. On the one hand, building hydrogen plants near hydropower plants with spillage can better utilize the otherwise curtailed hydropower and save electricity cost, but it may incur higher hydrogen transportation cost because many hydropower plants are in remote mountainous regions far from major demand regions. On the other hand, placing hydrogen plants near demand regions reduces hydrogen transportation cost, but it may lead to higher grid upgrade cost because electricity needs to be transmitted through the grid over a long distance.

We first describe electricity transmission using the DC power flow model, which is prevalent in the grid expansion planning literature (Latorre et al. 2003, Hemmati et al. 2013, O'Neill et al. 2013, Zhang et al. 2022). The transmission grid can be represented as an undirected graph denoted by $G(N, L)$, where N is the set of nodes (which may not necessarily coincide with the set of regions I) and L is the set of lines. Electric power for hydrogen production flows through this network under the Ohms and Kirchhoff laws. For each node $m \in N$, we use θ_m to denote its voltage angle, which is a decision variable. For each line $(m, n) \in L$, we use p_{mn} to denote the power flow for hydrogen production on this line and b_{mn} to denote its susceptance. Because the susceptance is determined by the physical structure and material properties of the capacitor, we regard b_{mn} as a parameter, and we set the power flow p_{mn} together with p^{c}_m, p^{h}_m, and p^{i}_m (introduced below) as decision variables. Note that p_{mn} can be positive or negative. If $p_{mn} > 0$, then power flows from m to n and vice versa. The DC power flow equation states that the power through a line (m, n) is proportional to the difference of the voltage angles of nodes m and n, which is

$$p_{mn} = b_{mn}(\theta_m - \theta_n), \quad \forall (m, n) \in L. \tag{14}$$

The power flows also satisfy the balance equation. That is, for each node, the total outflow through the lines plus the power consumption at this node equals the total inflow plus the power generation at this node, which yields the following constraint:

$$\sum_{\substack{n \in N: \\ (m,n) \in L}} p_{mn} + p^{\mathrm{c}}_m = \sum_{\substack{n \in N: \\ (n,m) \in L}} p_{nm} + p^{\mathrm{h}}_m + p^{\mathrm{i}}_m, \quad \forall m \in N, \tag{15}$$

where p^{c}_m is the power consumption of the hydrogen plant at node m, p^{h}_m is the power generated by hydropower plants at node m, and p^{i}_m is the power generated from other sources (e.g., coal-fired generation units) at node m. Notice that in our model, the power generation and transmission are only concerned with hydrogen production and that those for satisfying other base loads are omitted. This simplification is feasible because of the linearity of the DC power flow model.

Let decision variable z_m denote the capacity of the hydrogen plant built at node m. The total power consumed by the hydrogen plant is nonnegative, and it should not exceed its capacity:

$$0 \le p^{\mathrm{c}}_m \le z_m, \quad \forall m \in N. \tag{16}$$

The power generation of hydropower plants, p^{h}_m, is limited by its available capacity (i.e., the maximum capacity minus the current power output). Let g^{h}_m denote this available capacity of hydropower plants at node m. In our case study of Sichuan Province, the parameter g^{h}_m corresponds to the curtailed hydropower capacity, which is the difference between what the hydropower plant could have output and what it actually outputs. It follows that

$$0 \le p^{\mathrm{h}}_m \le g^{\mathrm{h}}_m, \quad \forall m \in N. \tag{17}$$

The power transmission for hydrogen production imposes an extra burden on the grid transmission capacity. To accommodate these extra power flows, parts of the transmission lines need to be reinforced. This infrastructure investment is particularly necessary where the transmission is already congested because of excessive hydropower outputs. It is worth noting that if the current transmission network possessed adequate capacity to supply hydrogen plants in demand regions, there would be neither hydropower curtailment nor the need to colocate hydrogen plants with hydropower sources. Our discussion revolves around the decision between expanding transmission capacity to enable more injection of hydropower that would otherwise be curtailed or alternatively, producing hydrogen on-site and subsequently transporting it to demand centers.

Let decision variable u_{mn} be the expanded capacity of line (m, n). Assuming that the lines are already strained by hydropower outputs (the case with nonstrained lines can also be easily incorporated but is less relevant to our problem), then the expanded capacity should be at least the absolute value of the power flow for hydrogen production on this line:

$$-u_{mn} \le p_{mn} \le u_{mn}, \quad \forall (m, n) \in L. \tag{18}$$

Lastly, we describe hydrogen production and transportation. Suppose that the hydrogen plant at node m supplies f_{mi} kg of hydrogen to region i per day and that ρ is the electricity-hydrogen conversion rate. Then, the daily power consumption of the plant at node m is related to its total hydrogen supply via the following equation:

$$\tau p^{\mathrm{c}}_m = \rho \sum_{i \in I} f_{mi}, \quad \forall m \in N, \tag{19}$$

where parameter τ is used to unify the timescale (i.e., $\tau = 24$ hours/day to convert hourly rates into daily rates).

The hydrogen transported to each region should meet its demand. That is,

$$D_i = \sum_{m\in N} f_{mi}, \quad \forall i \in I. \tag{20}$$

Recall that D_i is the hydrogen demand of region i and that the right-hand side is the sum of hydrogen supply from all hydrogen plants. Below, we discuss the integrated optimization model for the design of a hydrogen supply chain network, building upon the discussions presented earlier.

3.3. The Integrated Optimization Model

Recall that the goal of the planner is to design hydrogen infrastructures at the minimum cost that consists of infrastructure investment and operating cost, subject to the VMT target Constraint (13). Suppose that c_i^{r}, c_m^{p}, and c_{mn}^{u} are the annualized unit capacity costs of hydrogen refueling stations, hydrogen plants, and transmission line upgrades, respectively. Let c_m^{h} and c_m^{i} be the unit costs of electricity generated by hydropower plants and from other conventional sources, respectively. Let c_{mi}^{t} be the unit hydrogen transportation cost from node m to region i, and let $\xi = 365$ days/year be the factor that converts daily cost into yearly cost. The planning problem can first be formulated as a bilevel optimization problem:

$$\begin{aligned}
\min \quad & \sum_{i\in I} c_i^{\mathrm{r}} y_i + \sum_{m\in N} c_m^{\mathrm{p}} z_m + \sum_{(m,n)\in L} c_{mn}^{\mathrm{u}} u_{mn} \\
& + \xi\tau \sum_{m\in N} (c_m^{\mathrm{h}} p_m^{\mathrm{h}} + c_m^{\mathrm{i}} p_m^{\mathrm{i}}) + \xi \sum_{m\in N}\sum_{i\in I} c_{mi}^{\mathrm{t}} f_{mi} \\
\text{s.t.} \quad & (w_{tr})_{r\in R_t\cup\{0\}} = \arg\min_{\omega_{tr}\in\{0,1\}} \left\{ \sum_{r\in R_t} l_r \omega_{tr} + \bar{l}_t \omega_{t0} \right. \\
& \left. : \sum_{r\in R_t} \omega_{tr} + \omega_{t0} = 1; \omega_{tr} \le x_k, \ \forall k \in S_{tr} \right\}, \\
& \qquad\qquad \forall t \in T, \\
& \text{Constraints (2)–(3d), (6a)–(20),} \\
& \theta_m, p_m^{\mathrm{i}}, f_{mi} \ge 0, \quad \forall i \in I, m \in N.
\end{aligned} \tag{21}$$

In the above formulation, the objective is to minimize the total annualized cost, which includes the cost of building HRSs and hydrogen plants, the cost of transmission line upgrades, the cost of electricity, and the cost of hydrogen transportation. The lower level of the optimization problem considers the route choice and mode choice for each trip $t \in T$ as discussed in Problem (1). We extend the lower problem for each $t \in T$ as a Route-Choice-Integer Programming (RC-IP):

$$\begin{aligned}
\text{(RC-IP)} \quad \min \quad & \sum_{r\in R_t} l_r w_{tr} + \bar{l}_t w_{t0} && \text{(22a)} \\
\text{s.t.} \quad & \sum_{r\in R_t} w_{tr} + w_{t0} = 1, && \text{(22b)} \\
& w_{tr} \le x_k, \quad \forall r \in R_t, k \in S_{tr}, && \text{(22c)} \\
& w_{tr} \in \{0,1\}, \quad \forall r \in R_t \cup \{0\}. && \text{(22d)}
\end{aligned}$$

The dual problem, Route-Choice-Dual (RC-D), to the linear relaxation of (RC-IP), is given by

$$\begin{aligned}
\text{(RC-D)} \quad \max \quad & \lambda_t - \sum_{r\in R_t}\sum_{k\in S_{tr}} x_k \pi_{rk} && \text{(23a)} \\
\text{s.t.} \quad & l_r \ge \lambda_t - \sum_{k\in S_{tr}} \pi_{rk}, \quad \forall r \in R_t, && \text{(23b)} \\
& \bar{l}_t \ge \lambda_t, && \text{(23c)} \\
& \pi_{rk} \ge 0, \quad \forall r \in R_t, k \in S_{tr}. && \text{(23d)}
\end{aligned}$$

We provide the following lemma to characterize drivers' optimal route and mode choice.

Lemma 2. *Suppose all route lengths l_r are distinct. A feasible solution $(w_{tr})_{r\in R_t\cup\{0\}}$ to (RC-IP) is optimal if and only if there exists a feasible solution $(\lambda_t, (\pi_{rk})_{r\in R_t, k\in S_{tr}})$ to (RC-D) such that*

$$\sum_{r\in R_t} l_r w_{tr} + \bar{l}_t w_{t0} \le \lambda_t - \sum_{r\in R_t}\sum_{k\in S_{tr}} x_k \pi_{rk}. \tag{24}$$

As a consequence, we can use Condition (24) in Lemma 2 together with Constraints (22b)–(22d) in (RC-IP) and Constraints (23b)–(23d) in (RC-D) to define the optimal route choices by drivers. To deal with the bilinear term $x_k\pi_{rk}$ in (24), we further introduce auxiliary variable ψ_{rk} and replace (24) with the following constraints:

$$\begin{aligned}
& \sum_{r\in R_t} l_r w_{tr} + \bar{l}_t w_{t0} \le \lambda_t - \sum_{r\in R_t}\sum_{k\in S_{tr}} \psi_{rk}, && \text{(25a)} \\
& \psi_{rk} \ge 0, \quad \forall r \in R_t, k \in S_{tr}, && \text{(25b)} \\
& \psi_{rk} \le \pi_{rk}, \quad \forall r \in R_t, k \in S_{tr}, && \text{(25c)} \\
& \psi_{rk} \le M x_k, \quad \forall r \in R_t, k \in S_{tr}, && \text{(25d)} \\
& \psi_{rk} \ge \pi_{rk} - M(1 - x_k), \quad \forall r \in R_t, k \in S_{tr}, && \text{(25e)}
\end{aligned}$$

where M is a big constant. (In our case study in Section 4, we find that the choice of the M value does not bottleneck the computational efficiency, and thus, we simply set $M = 10^5$.)

Finally, the integrated optimization problem can be reformulated as the following mixed-integer second-order cone program, whose detailed formulation is deferred to Online Appendix B.2.1:

$$\begin{aligned}
\min \quad & \sum_{i\in I} c_i^{\mathrm{r}} y_i + \sum_{m\in N} c_m^{\mathrm{p}} z_m + \sum_{(m,n)\in L} c_{mn}^{\mathrm{u}} u_{mn} \\
& + \xi\tau \sum_{m\in N} (c_m^{\mathrm{h}} p_m^{\mathrm{h}} + c_m^{\mathrm{i}} p_m^{\mathrm{i}}) + \xi \sum_{m\in N}\sum_{i\in I} c_{mi}^{\mathrm{t}} f_{mi} \\
\text{s.t.} \quad & \text{Constraints (2)–(3d), (6a)–(20),} \\
& \text{Constraints (22b)–(22d), (23b)–(23d), (25a)–(25e),} \\
& \qquad\qquad \forall t \in T, \\
& \theta_m, p_m^{\mathrm{i}}, f_{mi} \ge 0, \quad \forall i \in I, m \in N.
\end{aligned} \tag{26}$$

In Problem (26), aside from the SOC Constraints (6) and (1), all other constraints and the objective function are

linear in the decision variables. This MISOCP formulation can be efficiently solved using optimization software, such as Gurobi, which supports branch-and-bound and interior point methods. For a thorough review of second-order cone programming, we refer readers to Alizadeh and Goldfarb (2003).

For the sake of clarity, our model development focuses on a single-period setting. Nevertheless, the trip demand of drivers and the available capacities of power plants in practice can vary on different timescales (e.g., hours, days, weeks, and months). To incorporate such variability over different time periods, the planner can extend the above formulation to a multiperiod model by setting a different set of relevant parameters and decision variables for each period. We present a detailed formulation for the multiperiod model in Online Appendix B.2.2.

4. Case Study of HFV Infrastructure Planning

In this section, we apply the integrated optimization model in Section 3 to the case of Sichuan Province in China and develop managerial insights on the dual benefit of reducing renewable energy curtailment and developing green transportation by promoting HFVs. We first describe the settings of our case study, and then, we study the following key questions. (i) What is the optimal infrastructure planning for the hydrogen supply chain under various VMT targets? (ii) What factors influence the efficiency of HFVs in reducing hydropower curtailment? (iii) Which option—HFVs or EVs—presents a more viable solution to attain the desired dual benefit?

4.1. Hydropower Curtailment and Power Transmission in Sichuan Province, China

Sichuan is a province located in southwest China with 21 prefecture-level cities and a total population of 83.68 million (in 2021). Figure 3(a) shows the map of the cities, which are numbered by their population in descending order. For example, city #1 (Chengdu) is the capital city of Sichuan Province, and it has the largest population and highest per capita gross domestic product. As we can see, the most populated cities are located in the eastern part of the province, which is called the Sichuan Basin, a lowland region surrounded by mountains on all sides.

Sichuan Province is also rich in hydropower. The installed hydropower capacity in Sichuan Province is over 76 GW, which accounts for about 80% of the total installed capacity and contributes more than 85% of electricity generation of the province (Sichuan Provincial Economic and Information Department 2020). The hydropower in Sichuan Province is most abundant from May to October when there is a large amount of rainfall. However, because of insufficient demand and limited transmission capacity, vast amounts of electricity curtailment often occur during these months. In 2016, over 11 TWh of hydropower was curtailed from May to October. Figure 3(b) illustrates the spatial distribution of hydropower curtailment in the electricity transmission network of Sichuan Province. However, different from Figure 3(a), where the majority of population is in the *eastern* part of Sichuan Province, Figure 3(b) shows that most of the curtailment happens in the *southwestern* region, where many hydropower plants are located in mountainous areas. Such a spatial mismatch between hydropower and population poses an immense challenge for curtailment reduction and HFV infrastructure planning.

In the case study, we consider the set of candidate regions I as the 21 prefecture-level cities in Sichuan Province shown in Figure 3(a). We consider long-haul transportation with at most two stops. The trip rate N_t for each $t \in T$ is estimated using the gravity model, which is a commonly used method in the transportation

Figure 3. (Color online) Population, Hydropower Curtailment, and the Transmission Grid in Sichuan Province

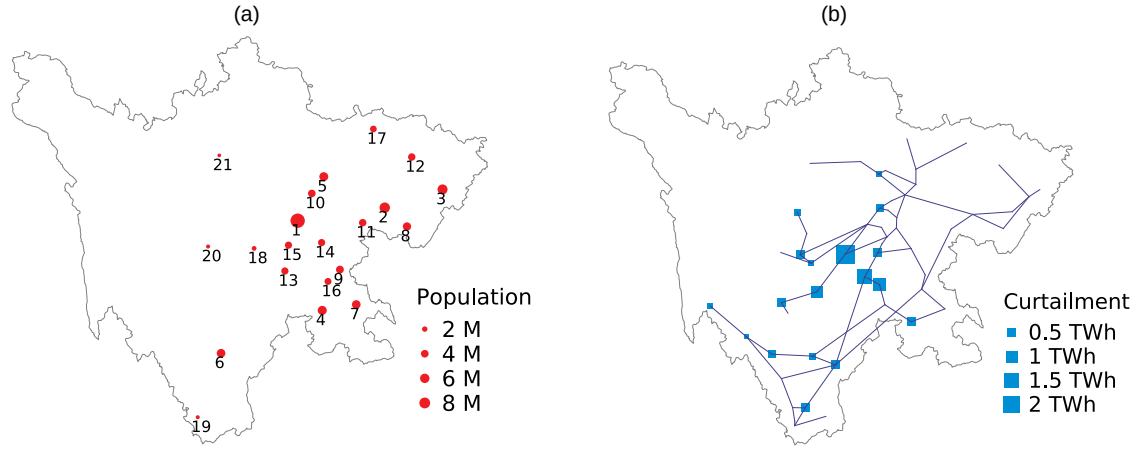

Notes. (a) Population. (b) Curtailment and transmission grid.

literature (e.g., Ortúzar and Willumsen 2011). Following a similar approach of He et al. (2017), we use the trip distributions as proxies to utility parameters $\boldsymbol{a}_i$, and we obtain their mean $\boldsymbol{\mu}_i$ and covariance matrices $\boldsymbol{\Sigma}_i$ from the gravity model regression. The aspiration levels b_i are set to be 0.9 for all cities. For details of the estimation procedure as well as other parameters about trips and hydrogen demand, see Online Appendix C.1.

For our grid network modeling, we use a unique and high-resolution grid data set from Sichuan Province including the structure and parameters of the high-voltage DC transmission grid. We also collect the data regarding the capacities and curtailment of the power plants in 2016. The original data set contains 234,386 entries, involving 1,402 nodes and 3,501 lines at the voltage levels of 500, 220, and 110 kV, and it includes detailed parameters of the grid, such as base load, generator capacity, and line impedance. For the scope of this work, we choose to focus on the 500-kV interregion transmission grid, which has 54 nodes and 67 lines, as illustrated by the lines in Figure 3(b). As mentioned above, the hydropower curtailment in Sichuan Province exhibits clear seasonality. Therefore, we consider the multiperiod model in our case study. Based on the monthly total curtailment data in Figure 4, we divide a year into four periods: May and June (period 1), July and August (period 2), September and October (period 3), and November to April (period 4). We set the available capacities of hydropower plants in each period to be the sum of the curtailed capacities. The multiperiod model minimizes the sum of the costs weighted by the length of each period. More details are available in Online Appendix B.2.2.

We obtain electricity costs from the Sichuan Electricity Market Report (Sichuan Power Exchange Center 2020). According to the report, the average market price of otherwise curtailed hydroelectricity is $c_m^{\mathrm{h}} = \$11.1$/megawatt-hour (MWh), and the average price of electricity directly purchased from the grid is $c_m^{\mathrm{i}} = \$66.5$/MWh. The cost parameters of infrastructures (HRS, hydrogen plant, and grid expansion) and hydrogen transportation are obtained from relevant literature and technical reports. The details are provided in Online Appendix C.1.5.

Figure 4. (Color online) Monthly Hydropower Curtailment

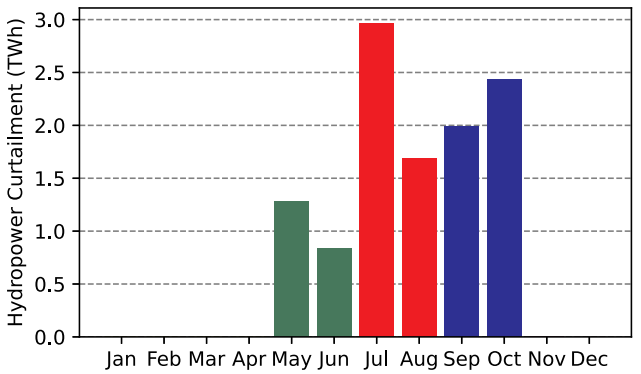

4.2. Proposed Infrastructure Design

We first investigate the optimal infrastructure design under different VMT targets. As described, the spatial distribution of hydropower curtailment and population in Sichuan Province exhibits an acute mismatch, which poses interesting questions regarding the design of the hydrogen supply chain network.

- Where should HRSs be built: in populous cities to promote HFV adoption or near hydropower curtailment sources to reduce hydrogen costs?
- Where should hydrogen plants be built: near hydropower curtailment nodes to save electricity and grid expansion costs or near demand regions to reduce transportation costs?

The answers to these questions may depend on the VMT target (i.e., the scale on which the planner wishes to promote HFVs). Therefore, we solve the optimization model with varying VMT targets Γ ranging from 10% to 90%. The computational time varies from 49 to 258 seconds across instances (implemented in Gurobi by utilizing an AMD EPYC 7643 48-Core Processor with 8 GB memory). Figure 5 shows four selected optimal infrastructure designs with low (10%, 30%) and high (50%, 70%) VMT targets, respectively. (The optimal designs under other VMT targets are available in Online Appendix C.2.)

The results show that *the optimal deployment of HRSs displays different spatial patterns under low and high VMT targets*. As the VMT target rises from 10%, the planning of HRSs and plants starts from the western part of Sichuan Province (e.g., cities #6 Liangshan, #18 Ya'an, #19 Panzhihua, #20 Ganzi, and #21 Aba in Figure 5, (a) and (b)) outside of the Sichuan Basin so that the hydropower curtailment near those regions can be locally utilized (that is, the HRSs and plants are nearby). This design also suggests some HRSs in the medium-sized cities on the outskirts of the Sichuan Basin (e.g., cities #10 Deyang, #13 Leshan, and #15 Meishan) because these cities have sizeable populations and are also not far away from nodes with hydropower curtailment (see Figure 5, (a) and (b)). Notably, in this case, the capital city Chengdu (#1) is not selected, although it has high trip demand.

When the target is high ($\Gamma \geq 50\%$), however, the capital city Chengdu (#1) emerges as the center of HFV trips and hydrogen consumption, with a significantly larger HRS capacity than other cities (see Figure 5, (c) and (d)). The high trip demand makes this capital city important to be selected for reaching the higher VMT target. Moreover, it is evident that in order to meet the higher VMT target, the design suggests the deployment of more HFV infrastructures (including both HRSs and plants) in large

Figure 5. (Color online) Optimal Infrastructure Designs Under Different VMT Targets

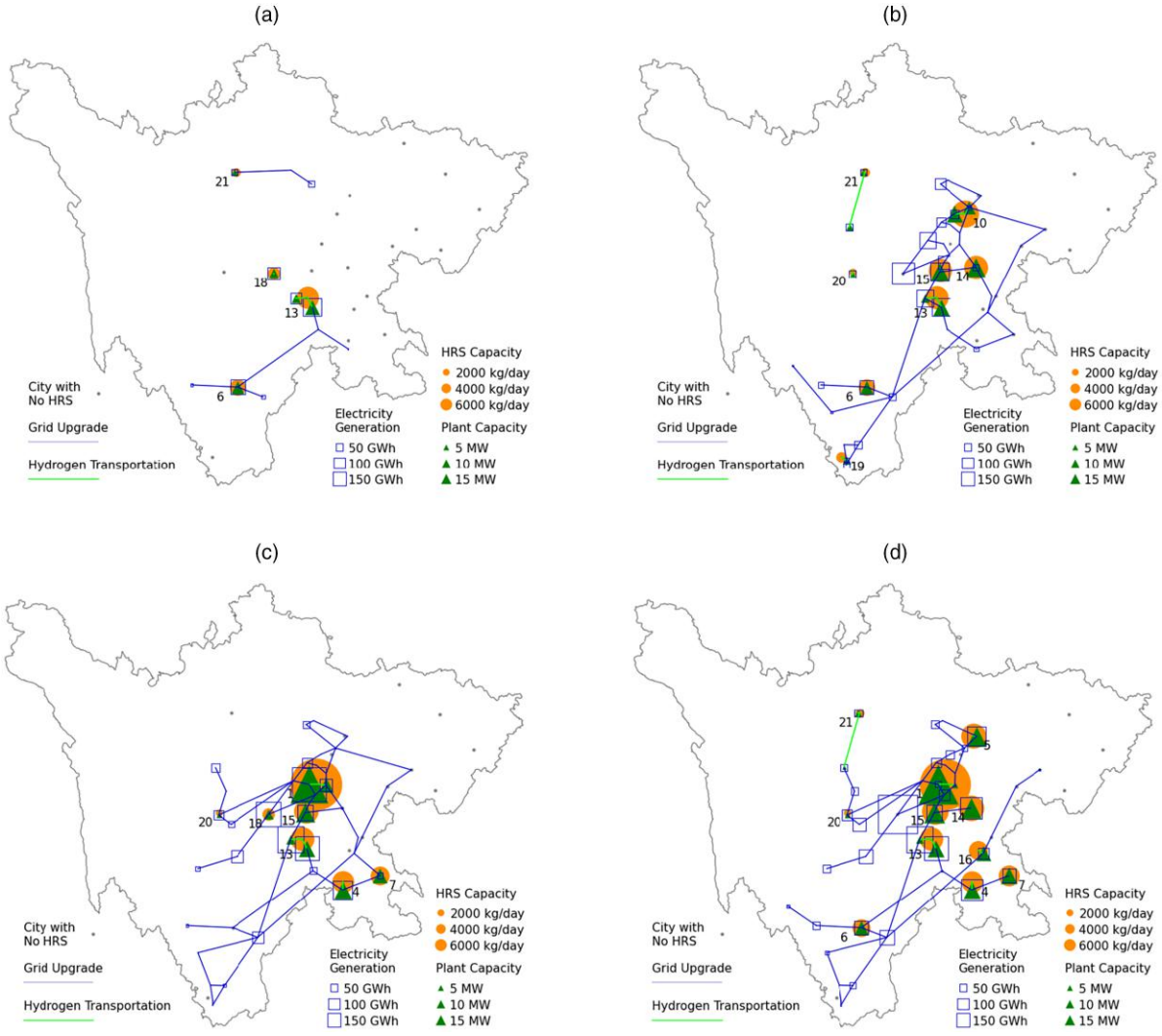

Notes. (a) Target Γ = 10%. (b) Target Γ = 30%. (c) Target Γ = 50%. (d) Target Γ = 70%.

cities inside the Sichuan Basin, which is centered at Chengdu. To make the hydrogen production (shown by the hydrogen plants) close to the hydrogen demand (shown by HRSs), as shown in Figure 5(d), for example, a great effort should be made to upgrade the grid transmission to bring the hydropower electricity to those hydrogen plants in those large cities. This is mainly because under the current cost estimates, it is more economical to use transmitted (otherwise, curtailed) hydropower or local nonrenewable sources of electricity for hydrogen production than to logistically transport hydrogen over long distances. Furthermore, we conduct additional numerical experiments and find that the optimal locations under one VMT target can be quite suboptimal under another VMT target (we omit details for brevity). These results verify that defining the VMT target is crucial for planning hydrogen infrastructure.

4.3. Effectiveness in Curtailment Reduction

As we have discussed above, besides developing greener transportation, promoting HFVs can be an effective means to reduce hydropower spillage. Because of its cheap price, the otherwise curtailed electricity can be used to produce hydrogen at low cost. This advantage has been highlighted in many strategic hydrogen plans (e.g., the hydrogen plan of Sichuan Province) (Sichuan Provincial Economic and Information Department 2020). Nevertheless, this cost advantage may be dampened by the fact that using the otherwise curtailed hydropower can entail costly grid upgrades or long-distance hydrogen transportation. In comparison, directly purchasing electricity from the grid (often generated from local nonrenewable sources) for hydrogen production incurs a higher marginal cost but on the other hand, avoids transmission grid upgrade because

the electricity is directly sourced at the node where the electricity is consumed.

Therefore, here we investigate which factors influence the efficiency of HFVs in reducing hydropower curtailment. For this purpose, we compute the total curtailment reduction $\xi\tau\sum_{m\in N}p_m^{\mathrm{h}}$ in the optimal solutions under different VMT targets, which we consider as the baseline scenario. Furthermore, we also consider three other scenarios by modifying parameters in the baseline: (1) doubling the grid upgrade cost c_{mn}^{u} only, (2) reducing the cost of electricity directly purchased from the grid (c_m^{i}) only, and (3) applying both modifications. The results are shown in Figure 6.

The results in Figure 6 show that *promoting the adoption of HFVs can overall help in reducing hydropower curtailment, but the extent varies by the grid upgrade cost and the electricity purchase cost*. In the baseline and the first alternative scenario (i.e., high grid upgrade cost), curtailment reduction shows a positive trend across all VMT values. We also observe that the higher grid upgrade cost generally hinders curtailment reduction because utilizing the otherwise curtailed hydropower becomes less favorable when the cost of the required transmission grid expansion increases. The magnitude of this hindrance, however, is not very large in the current parameter setting. On the other hand, when the cost of electricity from other sources is low (in the second and third alternative scenarios), curtailment reduction only increases marginally when the VMT target goes beyond 60%. This is because a moderate additional hydrogen demand is met mainly by using directly purchased electricity instead of otherwise curtailed hydropower. In this case, further pushing a high adoption rate for HFVs may not be too beneficial from the perspective of alleviating hydropower spillage. In summary, to achieve the dual benefit of reducing hydropower spillage and developing green transportation, the planner should carefully evaluate the relevant factors, such as grid upgrade cost and electricity purchase cost, and then, the planner should choose the right HFV adoption target.

Figure 6. (Color online) Evaluating the Effectiveness in Curtailment Reduction

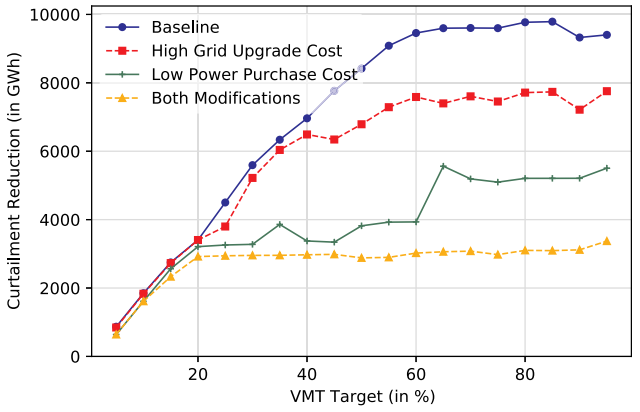

4.4. HFVs or EVs as a Viable Solution

There is an ongoing debate on the pros and cons of EVs and HFVs, both of which represent significant advancements in sustainable transportation technologies. HFVs excel in heavy-duty trucks and buses, whereas EVs dominate the personal and last-mile delivery sectors. For heavy-duty trucks, HFVs boast an impressive driving range of 500–800 km (Hyzon Motors 2023, Nikola 2023b), surpassing the typical range of 160–530 km (Nikola 2023a, Volvo Trucks 2023) achievable by EVs. The refueling/charging time also introduces a significant contrast. HFVs only take 5–20 minutes for refueling (Nikola 2023b) compared with the more time-consuming 90-plus minutes for EV charging (Nikola 2023a). Additionally, hydrogen can be transported to various locations, which allows for strategic placement of HRSs in locations distinct from hydrogen plant sites. In contrast, transporting batteries over long distances on a large scale is not practical, and electric charging stations are constrained to be sited where adequate power grid capacity is available. On the other hand, EVs have higher energy efficiency than HFVs. Note that EVs draw electricity directly from the grid to power the motor without additional energy conversion. In contrast, HFVs involve a more intricate process, including water electrolysis, hydrogen compression, and fuel consumption, as they transform electricity into hydrogen power for mileage. The distinctions between HFVs and EVs are outlined in Table 1.

To compare HFVs and EVs in terms of cost saving and curtailment reduction, we next examine various parameters for our case study. To mitigate the disparities in driving range and refueling/charging time, we set the driving ranges for both HFV and EV as 700 km and do not consider the refueling/charging time. Furthermore, energy efficiency for EVs is set as $\rho' = 1.2$ kilowatt-hours (kWh)/km (Yahoo Finance 2022), and energy efficiency for HFVs is 8.0 kg of hydrogen per 100 km as highlighted by McKinsey & Company (2022). The electrical energy needed to produce green hydrogen is quantified at 50 kWh/kg of hydrogen (Hydrogen Newsletter 2023). The transportation per kilogram via tube trailers incurs costs of \$7 per 1,000 km (Energy Technology Network 2014), and the cost via pipelines is projected to be \$0.3 per 1,000 km (Enlit 2022). Meanwhile, the cost dynamics of hydrogen production and refueling infrastructure come into focus. We estimate the cost of a hydrogen plant at \$400,000/MWh, based on values reported by (The Oxford Institute for Energy Studies 2022) in Jan 2022 (and adjusted for technological advancements). In the pursuit of efficient charging for EVs, WattEV constructs solar charging stations delivering 515 km of range to a Class 8 tractor in 30 minutes

Table 1. Comparison Between HFVs and EVs

Parameter	HFV	EV
Environmental impact	Zero emissions at the tailpipe; dependent on hydrogen production	Zero emissions at the tailpipe; dependent on electricity source and battery production
Main purposes	Heavy-duty trucks and buses	Personal and last-mile delivery vehicles
Driving range (heavy-duty trucks)	500–800 km	160–530 km
Refueling/charging time	5–20 minutes	>90 minutes
Vehicle efficiency	Lightweight fuel cell	Heavy battery
Refueling/charging location	Flexible infrastructure expansion	Grid-bound infrastructure
Energy efficiency	Low	High

(Clean Technica 2021), and they cost \$10 million to build. Additionally, Tesla is seeking nearly \$100 million from the United States to build nine electric semitruck charging stations along a route from the southern border of Texas to northern California (Bloomberg 2023). Therefore, in this study, we set the cost of a charging station for heavy-duty trucks as \$10 million, and we summarize key parameters in Table 2.

Note that we have 54 nodes in the transmission grid and 21 regions for candidate refueling stations. For ease of comparison, we assume that EV charging in each region can be provided from the nearest node of the transmission grid network at no cost. The planning problem for EV is then formulated as follows:

$$\begin{aligned} \min \quad & \sum_{i\in I} c^{\mathrm{r}}_i y_i + \sum_{(m,n)\in L} c^{\mathrm{u}}_{mn} u_{mn} + \xi\tau \sum_{m\in N} (c^{\mathrm{h}}_m p^{\mathrm{h}}_m + c^{\mathrm{i}}_m p^{\mathrm{i}}_m) \\ \text{s.t.} \quad & \text{Constraints (2)–(3d), (6a)–(18), (22b)–(22d),} \\ & \text{(23b)–(23d), (25a)–(25e),} \\ & \tau p^{c}_{m_i} = \rho' D_i/\eta, \qquad \forall i \in I, \\ & \theta_m, p^{\mathrm{i}}_m, f_{mi} \geq 0, \qquad \forall i \in I, m \in N. \end{aligned} \tag{27}$$

Recall that $\eta = 0.08$ kg/km represents the amount of hydrogen needed for each kilometer's drive and that D_i is the total hydrogen demand in region $i \in I$. We have D_i/η representing the demand in mileage needed at region i and $\rho' D_i/\eta$ as the required electric energy (megawatt-hours). We also remove $\xi \sum_{m\in N} \sum_{i\in I} c^{\mathrm{t}}_{mi} f_{mi}$ and $\sum_{m\in N} c^{\mathrm{p}}_m z_m$ from the objective of the HFV problem in (26) because there is no fuel transportation option or hydrogen plant construction involved for EV operations.

4.4.1. Efficiency Frontiers of HFV and EV. From a forward-looking perspective, it is expected that HFV transportation cost will be lowered (e.g., with the increasing availability of pipeline transportation). The construction cost for HRSs will also decrease. In this section, we examine how these cost factors impact the decision between HFVs and EVs as a viable solution for curtailment reduction. We establish an efficiency frontier by varying the hydrogen transportation cost and HRS construction cost, illustrated in Figure 7, for low (30%) and high (70%) VMT targets, respectively. To this end, we first solve for the minimum cost for promoting EVs from Problem (27). Subsequently, at each hydrogen transportation cost level, we identify the corresponding HRS cost under which the HFV Problem (21) implies the same total cost as the EV problem does.

From Figure 7, we observe that *EVs offer an advantage when the hydrogen transportation cost and/or HRS cost are higher. Furthermore, this advantage becomes more evident with a higher VMT target*, such as $\Gamma = 70\%$, potentially because of EV's higher energy efficiency in meeting higher energy demand. Consequently, EVs can be a favorable choice when the government aims for widespread adoption, especially under conditions of high HRS or hydrogen transportation costs. *However, HFVs prove to be more cost effective than EVs in the status quo under both VMT targets.* Recall that transporting hydrogen by tube trailer costs \$7 per kilogram per 1,000 km (Energy Technology Network 2014) and that the cost via pipelines is \$0.3 per 1,000 km (Enlit 2022). Based on the current estimate of HRS cost at \$1.9 million (U.S. Department of Energy 2020), HFVs are more cost effective at any reasonable hydrogen transportation cost level, as reported in Figure 7. Anticipated decreases in the

Table 2. Parameters for HFVs and EVs in the Case Study

Parameter	HFV	EV
Driving range (heavy-duty trucks)	700 km	700 km
Energy efficiency	50 kWh/kg, 8 kg/100 km	120 kWh/100 km
Fuel transportation cost per 1,000 km	Tube trailer \$7/kg; pipeline \$0.3/kg	Not available
Fuel production infrastructure cost	Hydrogen plant: \$400 k/MWh	—
Refueling/charging station cost	\$1.9 million	\$10 million

Figure 7. (Color online) Comparison Between EVs and HFVs on the Total Cost Under Different Hydrogen Transportation Costs and VMT Targets

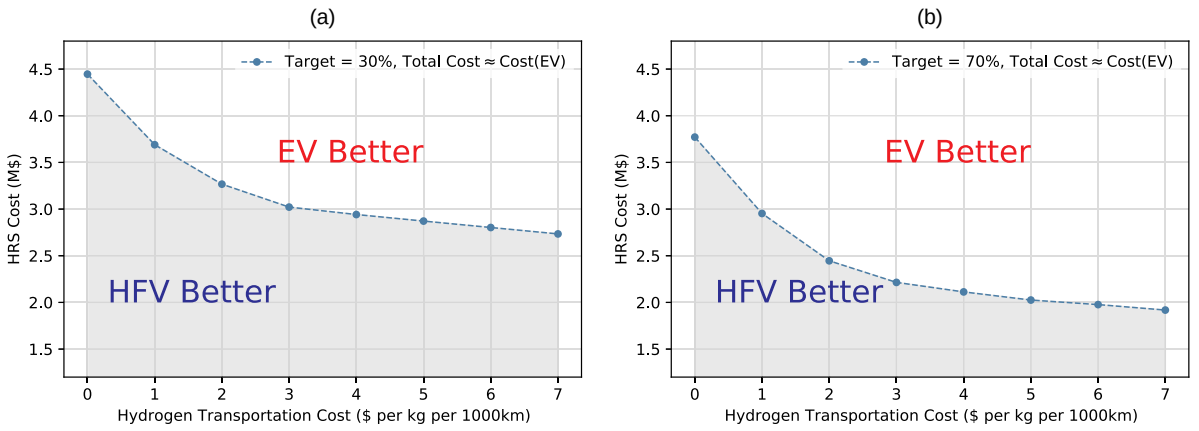

Notes. (a) Target $\Gamma = 30\%$. (b) Target $\Gamma = 70\%$.

hydrogen transportation cost (e.g., via pipelines) and the HRS cost are expected to generate more cost savings.

4.4.2. Performance Comparison Under Grid Constraints. Our system designs permit the import of electricity, which has the potential to compromise the goal of achieving 100% renewable energy usage as imported electricity may originate from coal sources. Thus, it is important to investigate the extent to which renewable energy can be utilized. Moreover, we also explore the optimal VMT targets that can be achieved without either electricity importation or grid upgrades.

Figure 8 displays the total costs incurred and the curtailment reduction achieved for HFVs and EVs when no grid upgrade is available but when the import of electricity is allowed. We notice that *the total costs of HFVs and EVs remain comparable across different VMT targets, whereas the total curtailment reduction for HFVs significantly exceeds that of EVs*. This discrepancy results from the increased flexibility that hydrogen's transportability makes possible. Hydrogen's transportability allows for the strategic placement of hydrogen plants near sources of curtailment, thereby facilitating better utilization of hydropower while allowing HRSs to be positioned in densely populated demand regions. In contrast, for EV charging, effectively utilizing the curtailed energy without grid upgrades is challenging. A significant portion of its energy needs to be sourced from imported electricity. On the other hand, the lower energy efficiency of HFVs requires more electricity to achieve VMT targets. As a result, the costs of purchasing electricity balance out the savings from the flexibility that hydrogen transportation offers.

To examine the possibility of a 100% renewable system, we further consider the models with no electricity imported or grid upgrade. During the dry season (i.e., period 4 in Figure 4), hydropower curtailment is nonexistent, whereas the demand for transportation remains

Figure 8. (Color online) Total Cost and Curtailment Reduction with No Grid Upgrade

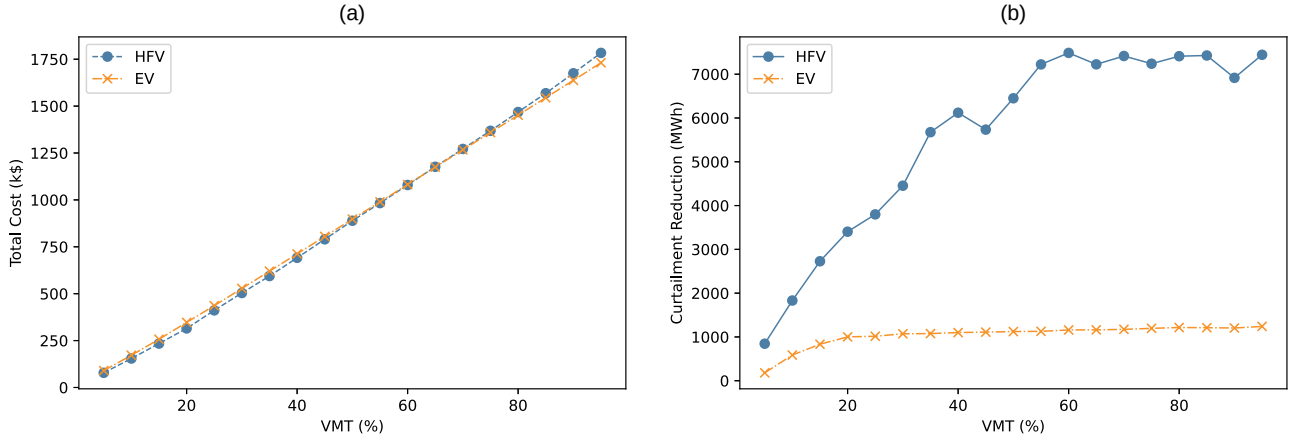

Notes. (a) Total cost. (b) Total curtailment reduction.

Figure 9. (Color online) Total Cost vs. VMT Target with No Grid Upgrade or Imported Electricity

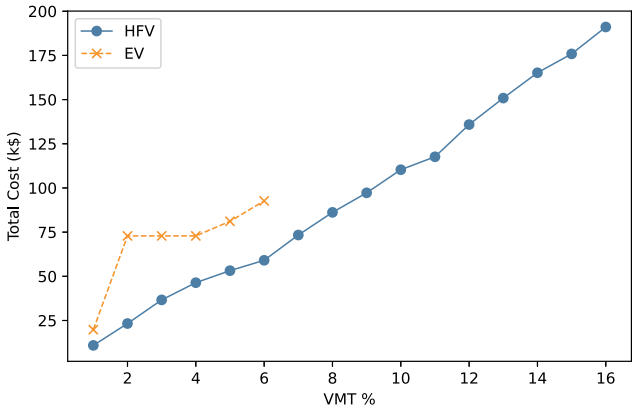

less affected by seasonal changes. Consequently, neither HFVs nor EVs can meet any positive VMT targets without the import of electricity. Suppose a peak-shaving method based on spillage adjustment (e.g., Abdelfattah et al. 2023) can transfer 10% of the curtailed power to the dry season such that a fully renewable system can be possible throughout the year. With the adjusted hydropower curtailment, we analyze the highest VMT targets that can be obtained by EVs and HFVs without grid upgrade or electricity import in Figure 9. We note that promoting EVs as a means to reduce energy curtailment incurs higher costs, and it can only achieve the VMT target up to a maximum of 6%. In contrast, the promotion of HFVs can achieve targets up to 16% at comparatively lower costs. The advantage of HFVs is also attributed to the flexibility provided by hydrogen transportation, leading to cost savings and enabling support for higher demand at dispersed locations. In summary, *HFVs outperform EVs in reducing curtailment in a renewables-dominant power system without the need for grid upgrade and can attain higher VMT targets than EVs, particularly in the face of seasonal variations in hydropower curtailment*.

5. Conclusion

HFVs have been proposed as a promising green transportation technology to help decarbonize the transportation sector and enable renewables to make a greater contribution to the energy systems. However, the lack of refueling infrastructure, the spatial mismatch between renewable energy sources and hydrogen demand, and the strained power transmission system all pose grand challenges to the promotion of HFVs. Solving these challenges requires a crossdisciplinary approach to account for important and interrelated factors in both transportation and power systems, such as drivers' vehicle adoption, hydrogen production and distribution, electricity transmission, and grid upgrade. To address these challenges, we propose an integrated model of transportation and power systems for planning supporting infrastructures. In particular, we explicitly model drivers' route choice and vehicle adoption that depends on HRS deployment. We also model the hydrogen supply chain, in which the electricity transmission and the grid upgrade are modeled using the DC power flow model. Using a distributionally robust optimization framework to address uncertainty in drivers' utility, our model can be reformulated as a computationally efficient MISOCP.

We apply our model to the case of Sichuan Province, where the vast amount of hydropower curtailment provides a great opportunity for promoting HFVs. Based on real data, our proposed solution suggests different infrastructure designs for different levels of the VMT target. Also, we evaluate the effectiveness of promoting HFVs in reducing hydropower curtailment, and we discuss relevant factors that affect the effectiveness, such as grid upgrade cost and electricity purchase price. In addition, we compare HFV and EV from various aspects; we see that EVs are advantageous under high hydrogen transportation cost and/or HRS cost, especially when the VMT target is high. However, HFVs are more cost effective under the current cost estimates, and this strength is likely to enhance with anticipated hydrogen-related cost reductions. Furthermore, when no grid upgrade or electricity import is permitted, HFVs outperform EVs in curtailment reduction by achieving higher VMT targets than EVs under seasonal variations in hydropower curtailment. Although this research primarily addresses promoting HFVs and reducing hydropower curtailment in Sichuan Province, our model can be potentially applied to other scenarios that involve other types of vehicles (e.g., plug-in electric vehicles) and energy sources (e.g., wind and solar).

To further bring out the potential of HFVs, several research questions are worth exploring. For example, our paper considers making up-front infrastructure planning decisions. However, as the HFV market is nascent and still developing, it will be desirable to consider an adaptive decision-making scheme for multistage infrastructure planning. In addition, although our work focuses on strategic decisions of designing the HFV infrastructure, it is also interesting to study optimizing the operations of HRSs and hydrogen plants together with real-time alternating current (AC) power grid control. Because our work takes the perspective of a central planner, one may alternatively consider the coordination between the grid operator, the hydrogen producer, and the refueling service provider as independent decision makers and study the implications. More broadly, our crossdisciplinary modeling framework may extend to synergize with other integrated supply chain design models for hydro and energy systems (e.g., Rafique et al. 2017, Wu and Ouyang 2017, Mun et al. 2021) toward building smart and connected infrastructures for the next generation.

Acknowledgments

The authors gratefully acknowledge Özlem Ergun (the department editor), the associate editor, and two anonymous referees for valuable review comments.

References

Abdelfattah AI, Shaaban MF, Osman AH, Ali A (2023) Optimal management of seasonal pumped hydro storage system for peak shaving. *Sustainability* 15(15):11973.

Alizadeh F, Goldfarb D (2003) Second-order cone programming. *Math. Programming* 95(1):3–51.

Alizadeh M, Wai HT, Chowdhury M, Goldsmith A, Scaglione A, Javidi T (2016) Optimal pricing to manage electric vehicles in coupled power and transportation networks. *IEEE Trans. Control Network Systems* 4(4):863–875.

Arslan O, Karaşan OE, Mahjoub AR, Yaman H (2019) A branch-and-cut algorithm for the alternative fuel refueling station location problem with routing. *Transportation Sci.* 53(4):1107–1125.

Avci B, Girotra K, Netessine S (2015) Electric vehicles with a battery switching station: Adoption and environmental impact. *Management Sci.* 61(4):772–794.

BAE Systems (2021) What is a hydrogen fuel cell truck? Accessed January 30, 2024, https://www.baesystems.com/en-us/definition/what-is-a-hydrogen-fuel-cell-truck.

Bhatti S, Lim M, Mak HY (2015) Alternative fuel station location model with demand learning. *Ann. Oper. Res.* 230(1):105–127.

Bloomberg (2023) Tesla wants to build a semi truck-charging route from Texas to California. (August 1), https://www.bloomberg.com/news/articles/2023-08-01/tesla-semi-truck-charging-route-pitched-at-100-million.

Brey JJ, Brey R, Carazo AF, Ruiz-Montero MJ, Tejada M (2016) Incorporating refuelling behaviour and drivers' preferences in the design of alternative fuels infrastructure in a city. *Transportation Res. Part C Emerging Tech.* 65:144–155.

Chen Q, Gu Y, Tang Z, Wang D, Wu Q (2021) Optimal design and techno-economic assessment of low-carbon hydrogen supply pathways for a refueling station located in shanghai. *Energy* 237:121584.

Clean Technica (2021) WattEV to break ground on solar charging station for heavy-duty trucks. Accessed December 15, 2021, https://cleantechnica.com/2021/09/15/wattev-to-break-ground-on-solar-charging-station-for-heavy-duty-trucks/.

Delage E, Ye Y (2010) Distributionally robust optimization under moment uncertainty with application to data-driven problems. *Oper. Res.* 58(3):595–612.

Dincer I (2012) Green methods for hydrogen production. *Internat. J. Hydrogen Energy* 37(2):1954–1971.

El Ghaoui L, Oks M, Oustry F (2003) Worst-case value-at-risk and robust portfolio optimization: A conic programming approach. *Oper. Res.* 51(4):543–556.

Energy Technology Network (2014) Hydrogen production & distribution. Accessed December 15, 2023, https://iea-etsap.org/E-TechDS/PDF/P12_H2_Feb2014_FINAL%203_CRES-2a-GS%20Mz%20GSOK.pdf.

Enlit (2022) Transporting hydrogen: When to pipe, ship, liquify or blend? Accessed December 15, 2023, https://www.enlit.world/hydrogen/the-hydrogen-trade-pipelines-and-ships/.

European Commission (2018) A clean planet for all: A European strategic long-term vision for a prosperous, modern, competitive and climate neutral economy. Accessed January 25, 2023, https://eur-lex.europa.eu/legal-content/EN/TXT/PDF/?uri=CELEX:52018DC0773.

European Commission (2020) A hydrogen strategy for climate-neutral Europe. Accessed December 15, 2021, https://eur-lex.europa.eu/legal-content/EN/TXT/?uri=CELEX:52020DC0301.

Glpautogas Info (2024) List of hydrogen refueling stations in China. Accessed January 25, 2023, https://www.glpautogas.info/data/hydrogen-stations-list-china.html.

He L, Ma G, Qi W, Wang X (2021) Charging an electric vehicle-sharing fleet. *Manufacturing Service Oper. Management* 23(2):471–487.

He L, Mak HY, Rong Y, Shen ZJM (2017) Service region design for urban electric vehicle sharing systems. *Manufacturing Service Oper. Management* 19(2):309–327.

Hemmati R, Hooshmand RA, Khodabakhshian A (2013) State-of-the-art of transmission expansion planning: Comprehensive review. *Renewable Sustainable Energy Rev.* 23:312–319.

Hydrogen Newsletter (2023) FAQs—General green hydrogen knowledge. Accessed December 15, 2023, https://www.hydrogennewsletter.com/faq-general-green-hydrogen-knowledge/.

Hyzon Motors (2023) Zero emission hydrogen fuel cell vehicles. Accessed December 15, 2023, https://www.hyzonmotors.com/.

International Renewable Energy Agency (2021) Policies for green hydrogen. Accessed July 27, 2024, https://www.irena.org/Energy-Transition/Policy/Policies-for-green-hydrogen.

Kang JE, Recker W (2015) Strategic hydrogen refueling station locations with scheduling and routing considerations of individual vehicles. *Transportation Sci.* 49(4):767–783.

Kim JG, Kuby M (2012) The deviation-flow refueling location model for optimizing a network of refueling stations. *Internat. J. Hydrogen Energy* 37(6):5406–5420.

Kuby M, Lim S (2005) The flow-refueling location problem for alternative-fuel vehicles. *Socio-Economic Planning Sci.* 39(2):125–145.

Kuby M, Lim S (2007) Location of alternative-fuel stations using the flow-refueling location model and dispersion of candidate sites on arcs. *Networks Spatial Econom.* 7(2):129–152.

Latorre G, Cruz RD, Areiza JM, Villegas A (2003) Classification of publications and models on transmission expansion planning. *IEEE Trans. Power Systems* 18(2):938–946.

Mahmutoğulları Ö, Yaman H (2023) Robust alternative fuel refueling station location problem with routing under decision-dependent flow uncertainty. *Eur. J. Oper. Res.* 306(1):173–188.

Mak HY, Rong Y, Shen ZJM (2013) Infrastructure planning for electric vehicles with battery swapping. *Management Sci.* 59(7):1557–1575.

McKinsey & Company (2022) Unlocking hydrogen's power for long-haul freight transport. Accessed December 15, 2023, https://www.mckinsey.com/capabilities/operations/our-insights/global-infrastructure-initiative/voices/unlocking-hydrogens-power-for-long-haul-freight-transport.

Mun KG, Zhao Y, Rafique RA (2021) Designing hydro supply chains for energy, food, and flood. *Manufacturing Service Oper. Management* 23(2):274–293.

Nikola (2023a) TRE BEV. Tech giant. Accessed December 15, 2023, https://nikolamotor.com/the-nikola-tre-bev-reinventing-short-haul-transportation/.

Nikola (2023b) TRE FCEV. All science. No fiction. Accessed December 15, 2023, https://www.nikolamotor.com/tre-fcev/.

O'Neill RP, Krall EA, Hedman KW, Oren SS (2013) A model and approach to the challenge posed by optimal power systems planning. *Math. Programming* 140:239–266.

Ortúzar JdD, Willumsen LG (2011) *Modelling Transport* (John Wiley & Sons, Hoboken, NJ).

Qi W, Sha M, Li S (2022) When shared autonomous electric vehicles meet microgrids: Citywide energy-mobility orchestration. *Manufacturing Service Oper. Management* 24(5):2389–2406.

Qi W, Zhang Y, Zhang N (2023) Scaling up electric-vehicle battery swapping services in cities: A joint location and repairable-inventory model. *Management Sci.* 69(11):6855–6875.

Rafique R, Mun KG, Zhao Y (2017) Designing energy supply chains: Dynamic models for energy security and economic prosperity. *Production Oper. Management* 26(6):1120–1141.

Sichuan Power Exchange Center (2020) Sichuan electricity market annual report. Accessed June 15, 2021, https://shoudian.bjx.com.cn/html/20210408/1146182.shtml.

Sichuan Provincial Economic and Information Department (2020) Sichuan hydrogen industry development plan. Accessed June 15, 2021, https://jxt.sc.gov.cn/scjxt/wjfb/2020/9/21/12979ab0d1cf41b18489d7d9559e4abf.shtml.

Simon HA (1957) *Models of Man: Social and Rational* (Wiley, New York).

Sixth Tone (2022) How the lights went off in China's hydropower capital. (September 21), https://www.sixthtone.com/news/1011262.

Stott B, Jardim J, Alsaç O (2009) DC power flow revisited. *IEEE Trans. Power Systems* 24(3):1290–1300.

The Oxford Institute for Energy Studies (2022) Cost-competitive green hydrogen: How to lower the cost of electrolysers? Accessed July 27, 2024, https://www.oxfordenergy.org/wpcms/wp-content/uploads/2022/01/Cost-competitive-green-hydrogen-how-to-lower-the-cost-of-electrolysers-EL47.pdf.

Timperley J (2021) When it comes to buses, will hydrogen or electric win? (December 9), https://www.wired.co.uk/article/future-buses-hydrogen-electric.

Toyota (2022) Trucking World endorses Toyota's hydrogen-powered fuel cells as a step toward a cleaner planet. Accessed January 30, 2024, https://pressroom.toyota.com/trucking-world-endorses-toyotas-hydrogen-powered-fuel-cells-as-a-step-toward-a-cleaner-planet/.

U.S. Department of Energy (2020) The Department of Energy hydrogen program plan. Accessed December 15, 2021, https://www.hydrogen.energy.gov/roadmaps_vision.html.

U.S. Department of Energy (2021) Fuel cell electric vehicles. Accessed June 15, 2021, https://afdc.energy.gov/vehicles/fuel_cell.html.

Volvo Trucks (2023) Volvo presents electric trucks with longer range. Accessed December 15, 2023, https://www.volvotrucks.com/en-en/news-stories/press-releases/2023/jun/volvo-presents-electric-trucks-with-longer-range.html.

Wu OQ, Ouyang Y (2017) Supply chain design and optimization with applications in energy industry. Terlaky T, Anjos MF, Ahmed S, eds. *Advances and Trends in Optimization with Engineering Applications* (Society for Industrial & Applied Mathematics, Philadelphia), 16–39.

Xinhuanet (2022) China maps 2021–2035 plan on hydrogen energy development. Accessed April 15, 2022, https://english.news.cn/20220323/428eaeae2c0a41b98ffb8d5ef4e91190/c.html.

Yahoo Finance (2022) Tesla semi unveiled with tri-motor setup, megawatt charging tech. Accessed December 15, 2023, https://finance.yahoo.com/news/tesla-semi-unveiled-with-tri-motor-setup-megawatt-charging-tech-121619247.html.

Yang L, Zhang J, Poor HV (2014) Risk-aware day-ahead scheduling and real-time dispatch for electric vehicle charging. *IEEE Trans. Smart Grid* 5(2):693–702.

Yao W, Zhao J, Wen F, Dong Z, Xue Y, Xu Y, Meng K (2014) A multi-objective collaborative planning strategy for integrated power distribution and electric vehicle charging systems. *IEEE Trans. Power Systems* 29(4):1811–1821.

Zhang Y, Lu M, Shen S (2021) On the values of vehicle-to-grid electricity selling in electric vehicle sharing. *Manufacturing Service Oper. Management* 23(2):488–507.

Zhang H, Qi W, Hu Z, Song Y (2017) Planning hydrogen refueling stations with coordinated on-site electrolytic production *2017 IEEE Power Energy Soc. General Meeting* (IEEE, Piscataway, NJ), 1–5.

Zhang N, Jiang H, Du E, Zhuo Z, Wang P, Wang Z, Zhang Y (2022) An efficient power system planning model considering year-round hourly operation simulation. *IEEE Trans. Power Systems* 37(6):4925–4935.